



Published in final edited form as:

*Nucl Med Biol.* 2006 November ; 33(8): 1055–1063.

## Induction of Apoptosis in Human Tumor Cells after Exposure to Auger Electrons: Comparison with Gamma-Ray Exposure

Tetsuro Urashima<sup>†</sup>, Hatsumi Nagasawa<sup>‡</sup>, Ketai Wang<sup>†</sup>, S. James Adelstein<sup>†</sup>, John B. Little<sup>§</sup>, and Amin I. Kassir<sup>†,\*</sup>

<sup>†</sup> Department of Radiology, Harvard Medical School, Boston, MA 02115, USA;

<sup>‡</sup> Department of Radiological Science, Colorado State University, Fort Collins, CO 80523, USA; and

<sup>§</sup> Department of Radiation Biology, Harvard School of Public Health, Boston, MA 02115, USA

### Abstract

To clarify the contribution of apoptosis to cell death in four human solid-tumor cell lines, clonogenic cell survival (indicator of radiosensitivity) and induction of caspase-3 and production of DNA fragmentation (markers for apoptosis) were studied in RKO, LS174T, MCF7, and TE671 cells exposed to DNA-incorporated, Auger-electron-emitting <sup>125</sup>I (5-[<sup>125</sup>I]iodo-2'-deoxyuridine) or  $\gamma$ -radiation. Clonogenic survival was assessed by the colony-forming assay, caspase-3 induction with a fluorogenic substrate, and DNA fragmentation by ligation-mediated PCR. For <sup>125</sup>I, the log dose-survival curves had no shoulder (high-LET-like) and decreased exponentially at different rates in various cell lines. Induction of caspase-3 in radiosensitive RKO and LS174T cells was 3-fold greater than in radioresistant TE671 and MCF7 cells. Nucleosomal laddering in <sup>125</sup>I-radioresistant cell lines was dose-dependent, and no laddering was detected in radioresistant lines. For  $\gamma$ -radiation, the survival curve for LS174T cells was monoexponential, and that for the other lines exhibited a distinct shoulder (low-LET-like). The most radiosensitive cell line, LS174T, showed the highest induction of CASP-3, and the most radioresistant line, TE671, the lowest. Although DNA laddering was not detectable in TE671 cells, it was observed in the other lines, being most prominent in LS174T cells. We conclude that apoptosis initiated by DNA-incorporated <sup>125</sup>I is dose-dependent, correlates with radiation sensitivity, and takes place through the CASP-3-mediated pathway, whereas that after  $\gamma$ -irradiation probably occurs via CASP-3-independent and/or CASP-3-mediated pathways and does not correlate with cell radiosensitivity.

### Keywords

apoptosis; tumor radiobiology; Auger electrons

### Introduction

Apoptosis, a programmed energy-dependent cellular suicide process occurring after exposure of cells to normal or pathologic stimuli, is characterized by chromatin condensation and DNA fragmentation into nucleosomal units, followed by membrane blebbing, and cell shrinkage [1]. It is generally accepted that radiation-induced apoptosis is a phenomenon dependent on cell type, dose, and time after  $\gamma$ -irradiation [2]. The target may be the plasma membrane, the cell nucleus, or both. Although many factors have been shown to affect the cellular response to ionizing radiation, the target lesion for radiation-induced apoptosis and the signaling

\*Address correspondence to Amin I. Kassir, Ph.D., Harvard Medical School, 200 Longwood Avenue, Armenise Building, Boston, MA 02115, USA; telephone: 617-432-7777, fax 617-432-2419, e-mail amin\_kassir@hms.harvard.edu..

pathway leading to the induction of apoptosis, especially following low-energy-electron irradiation of DNA, are still poorly understood. The comprehension of the mechanisms underlying such phenomena is essential, especially in order to maximize the effectiveness of radiotherapies delivered by external beams or in the form of targeted radionuclides.

Whatever triggers the death signal in apoptosis, DNA fragmentation is carried out via a signaling pathway that leads to the recruitment and activation of caspases, a family of cysteine-containing, aspartate-specific proteases [3–6]. Caspases may be divided into two functional subfamilies: initiator caspases, which are involved in upstream regulatory events, and effector caspases, which are directly responsible for cell disassembly events. Caspase-3 (Casp-3) is one of the latter “executioner caspases.” Active caspase-3 cleaves cellular substrates including DNA-PK (DNA-dependent protein kinase), PARP (poly(ADP-ribose) polymerase), DNA fragmentation factor, and  $\alpha$ -fodrin, and this process results directly in DNA fragmentation [6–11]. Datta et al. [12] have demonstrated in myeloid leukemia cells that ionizing  $\gamma$ -radiation-induced apoptosis is triggered by caspase-3, and this pathway to cell death differs from that of TNF (tumor necrosis factor)- or Fas-mediated cell death. Yu and Little [13] have shown in a lymphoblastic cell line that  $\gamma$ -radiation-induced apoptosis is initiated by a mechanism involving the caspase-3 cascade through both p53-dependent and -independent pathways. Jänicke et al. [14] have observed TNF- or staurosporine-induced apoptosis in MCF7 carcinoma cells (defective in exon 3 of the *caspase-3* gene) in which there is neither DNA fragmentation nor cellular shrinkage and membrane blebbing, implying that a caspase-3-independent pathway is activated.

It has been widely reported that thymocytes, lymphoid cells, and myeloid cells are susceptible to  $\gamma$ -radiation-induced apoptosis [13,15–21], but there are few investigations of human carcinomatous or sarcomatous cell lines. To clarify the possible contribution of apoptosis to cell death, we have compared the induction of caspase-3 and the production of DNA fragmentation in four such human tumor-cell lines exposed to DNA-incorporated iodine-125 ( $^{125}\text{I}$ ), a radionuclide whose decay leads to the emission of  $\sim 21$  very low energy, short-range ( $< 1 \mu\text{m}$ ) electrons (energy deposition mainly in DNA) [22–25] or to  $\gamma$ -radiation (energy deposition throughout the whole cell).

## Materials and methods

### Cell lines

The following cell lines were used: RKO (human colon adenocarcinoma), LS174T (human colon adenocarcinoma), MCF7 (human breast adenocarcinoma), and TE671 (human rhabdomyosarcoma). All four cells lines were cultivated in Eagle’s MEM (Gibco) supplemented with heat-inactivated FBS (10%), penicillin (100 units/ml), and streptomycin (100  $\mu\text{g/ml}$ ).

### Clonogenic survival after $^{125}\text{I}$ dUrd exposure and $\gamma$ -irradiation (colony-forming assay)

For clonogenic survival after  $\gamma$ -ray exposure, the cells were maintained in exponential growth in monolayer cultures with regular medium changes. The medium was renewed one day prior to  $^{137}\text{Cs}$   $\gamma$ -ray-source irradiation at a dose rate of 2.5 Gy/min. Cell survival was determined by a standard colony-formation assay; cell numbers were adjusted to yield approximately 50–100 viable colony-forming cells/100-mm Petri dish. We used two different numbers of cells (three Petri dishes for each set) to determine survival fraction at each experimental point. These dishes were incubated for 10 to 14 days, then fixed with 95% ethanol and stained with 0.1% crystal violet. Macroscopic colonies were counted and the survival fraction was calculated.

For clonogenic survival after 5-[<sup>125</sup>I]iodo-2'-deoxyuridine (<sup>125</sup>IdUrd) exposure, cells growing logarithmically in T-75 flasks with Eagle's MEM (supplemented as above) were trypsinized, and  $2 \times 10^5$  cells were plated per T-25 flask and incubated overnight at 37°C. Various concentrations of <sup>125</sup>IdUrd (3.7–37 kBq/ml) were then added to the flasks, and the cells were incubated a further 48 h. After exposure to <sup>125</sup>IdUrd, the cells were washed with PBS, trypsinized, and plated in Petri dishes that were cultivated for 10 to 14 days; the plates were then stained, and the cell colonies were counted as above. To measure DNA-incorporated <sup>125</sup>I, 100- $\mu$ l aliquots in triplicate of the trypsinized cell suspensions were precipitated with ice-cold 10% trichloroacetic acid on Gelman glass-fiber filters (type A/E, 25 mm) and counted in a Packard Auto-Gamma 500 counter.

### **Caspase-3/caspase-3-like protease induction after <sup>125</sup>IdUrd exposure and $\gamma$ -irradiation**

Caspase-3 induction was assayed using the PhiPhiLux-G<sub>1</sub>D<sub>2</sub> kit (Medical and Biological Laboratories Company, Ltd., Nagoya, Japan), which contains a fluorogenic substrate for caspase-3 and caspase-3-like proteases (CASP-3) in living cells. Logarithmically growing cells were trypsinized and  $5 \times 10^4$  cells were plated in 8-well chamber slides and cultivated overnight at 37°C. <sup>125</sup>IdUrd (0–185 kBq/ml) was added to the medium, and the CASP-3-positive cells were counted 3, 6, 24, 30, and 48 h from the beginning of incubation (0 time) according to the manufacture's protocol. Briefly, after exposure to a fluorogenic substrate solution, cells were washed with PBS, and cells with CASP-3-induction were observed under the fluorescence microscope. At least three fields were randomly selected, and the number of CASP-3-positive cells was counted. At the same time, DNA incorporation of <sup>125</sup>IdUrd at each time point was assayed as described above.

For measurement of CASP-3 induction after  $\gamma$ -ray exposure, cells were cultivated under the same conditions as for the colony-forming assay and were irradiated with a single dose of 0, 2.5, 5 or 10 Gy. After irradiation, the cells were incubated with a fluorogenic substrate solution, and those positive for CASP-3 were counted as described above.

### **Ligation-mediated PCR for detection of DNA fragmentation after <sup>125</sup>IdUrd exposure and $\gamma$ -irradiation**

RKO, LS174T, TE671 and MCF7 cells were cultivated with <sup>125</sup>IdUrd-containing medium (9.25, 18.5 and 37 kBq/ml) for 48 h. DNA extraction was carried out 6 h later with the DNA Extraction Kit (Stratagene, La Jolla, California), and the DNA was used for LM-PCR. In addition, the same cell lines were exposed to 5 and 10 Gy of  $\gamma$ -radiation and DNA was extracted 6 h later. The DNA of unirradiated cells was used as a control.

Ligation-mediated PCR for detecting DNA fragmentation was performed using the ApoAlert LM-PCR Ladder Assay kit (Clontech Laboratories, Incorporated, Palo Alto, California). Briefly, adaptor-ligated DNA (100 ng) was prepared and added to 10X LM-PCR Mix (10  $\mu$ l) and 50X Advantage cDNA Polymerase Mix (2  $\mu$ l) in a total volume of 100  $\mu$ l. The PCR was performed on a GenAmp 9700 Thermocycler (Applied Biophysics, Foster City, California): initial denaturation step at 72°C (8 min), followed by 94°C (1 min), 72°C (3 min)  $\times$  20 cycles, final extension step 72°C (15 min). Each 10- $\mu$ l amplified DNA sample was electrophoresed on 1.2% agarose/ETBr gel at 6 V/cm for 2.5 h. Samples of 100 bp were used as a standard to determine DNA fragment size.

## **Results**

### **Clonogenic survival after <sup>125</sup>IdUrd exposure and $\gamma$ -irradiation**

Clonogenic survival of the four cell lines grown for 48 h with various concentrations of <sup>125</sup>IdUrd is shown in Figure 1. With all cell lines, the log dose–survival plot decreases

linearly (high-LET-like). RKO and LS174T cell lines are more radiosensitive to  $^{125}\text{I}$ dUrd exposure than TE671 and MCF7 cell lines. The doses required to reduce survival to 37% ( $D_0$  values) are  $0.47\pm 0.04$  mBq/cell in RKO cells,  $0.69\pm 0.06$  mBq/cell in LS174T cells,  $1.45\pm 0.11$  mBq/cell in TE671 cells, and  $2.98\pm 0.33$  mBq/cell in MCF7 cells (Table I).

Survival curves for all four cell lines after  $\gamma$ -irradiation are shown in Figure 2. The curve for LS174T cells is of the high-LET type, whereas those for the other cell lines are low-LET-like with distinct shoulders. The  $D_0$  values are  $0.98\pm 0.01$  Gy in LS174T cells,  $0.77\pm 0.05$  Gy in TE671 cells,  $0.84\pm 0.05$  Gy in RKO cells, and  $1.15\pm 0.06$  Gy in MCF7 cells (Table II).

### Caspase-3/caspase-3-like protease induction after $^{125}\text{I}$ dUrd exposure and $\gamma$ -irradiation

Caspase-3/caspase-3-like protease (CASP-3) is rapidly (within 6 h) and highly (~30%) induced by the decay of DNA-incorporated  $^{125}\text{I}$  in a dose-dependent fashion in the two cell lines most sensitive to  $^{125}\text{I}$  irradiation (RKO and LS174T cells) (Figs. 3 and 4, Table I), but not in the radioresistant TE671 cells or the MCF7 cells (a cell line that has a functional *caspase-3* deletion) even when these latter are exposed to high concentrations of  $^{125}\text{I}$ dUrd (Fig. 4). For example, RKO cells have pronounced CASP-3 expression at  $^{125}\text{I}$ dUrd concentrations of 18.5 kBq/ml and higher, whereas MCF7 cells lack CASP-3 expression even at 185 kBq/ml. Furthermore, at a high dose of  $^{125}\text{I}$ dUrd (37 kBq/ml), CASP-3 levels increase sharply in RKO and LS174T cells at 6 h and remain high thereafter (up to 48 h), while a much less pronounced increase is seen in TE671 and MCF7 cells (Fig. 3). Finally, the DNA-incorporated activities of  $^{125}\text{I}$  needed to induce these high levels of caspase-3 in the RKO and LS174T cells are substantially less than those that produce low levels of caspase-3 in the other two cell lines (Fig. 4).

For  $\gamma$ -irradiation, CASP-3 expression increases sharply 1 h post irradiation of all four cell lines and then seems to level off (Fig. 5). The induction of this enzyme occurs in a dose-dependent manner (Fig. 6). Although the MCF7 cell line is defective in the expression of the *caspase-3* gene, notable immunofluorescence activities (12.0%) are detected (Table II). As the immunofluorescence assay for CASP-3 can detect the activities of both caspase-3 and caspase-3-like proteases, in MCF7 cells the positive signal is likely to be caused by the activity of caspase-3-like proteases.

### Ligation-mediated PCR for detection of DNA fragmentation

Figure 7 shows the detection of DNA fragmentation by the gel electrophoresis of LM-PCR products (20  $\mu\text{l}$ ). With both low and higher DNA-incorporated doses of  $^{125}\text{I}$ dUrd, prominent nucleosomal ladders (~180 bp apart) are present in LS174T and RKO cells (Fig. 7), and the signals for DNA fragmentation become stronger with increasing dose. However, no nucleosomal ladders are observed in DNA samples obtained from TE671 and MCF7 cells even when very high DNA-incorporated  $^{125}\text{I}$  activities are used (e.g. 70.3 mBq/cell). These results are consistent with the data from CASP-3 induction and, taken together with the findings of the colony-forming assay after  $^{125}\text{I}$ dUrd exposure (Table I), indicate that apoptotic cell death is induced both highly and dose dependently in sensitive cells but not in the more radioresistant cell lines.

After  $\gamma$ -irradiation of 5 and 10 Gy (Fig. 8), nucleosomal ladders ~180 bp apart are clearly discernible in LS174T, RKO and MCF7 cells, and the signal is stronger in DNA from cells treated with 10 Gy. In addition, DNA fragmentation in LS174T cells is more prominent than in RKO and MCF7 cells. However, no ladder is detectable in TE671 DNA. These results are in accord with the data on caspase-3/caspase-3-like protease induction and seem to be associated with the radiosensitivities to  $\gamma$ -radiation ( $D_0$  values) of the four cell lines, even though the correlation is not so obvious as that seen post  $^{125}\text{I}$  decay.

## Discussion

Auger electron emission from radioactive atoms such as iodine-125 occurs whenever an inner shell vacancy is created. These primary vacancies can be induced by electron capture or internal conversion. The highly excited residual atom de-excites with the emission of several (3–5) to many (30–50) low-energy electrons (Auger, Coster-Kronig, and super Coster-Kronig transitions) or atomic X-rays. Monte Carlo calculations, performed to determine the electron spectra of such radionuclides [22,23], have shown them to be extremely complex and to consist primarily of electrons with subcellular ranges. For  $^{125}\text{I}$ , the average Auger and Coster-Kronig electron spectra give a total of about 21 electrons per decay with energies ranging from approximately 15 eV to 24 keV [22,23,26]. The ejection of these electrons results in the deposition of a concentrated amount of energy (equivalent to  $10^4$ – $10^7$  Gy/decay) in an extremely small volume around the decay site, typically on the order of a few cubic nanometers [24–26]. The highly localized nature of energy absorption leads to severe damage of molecular structures only in the immediate vicinity of the decaying atom [27–30]. *In vitro* studies at the molecular and cellular levels have repeatedly demonstrated (i) the very high toxicity and efficient double-strand-break (DSB) formation when such radionuclides decay in close proximity to nuclear DNA [24,31–34], and (ii) the relative ineffectiveness of these radionuclides when the decay occurs in the cytoplasm or outside the cell [25,35,36]. In comparison,  $\gamma$ -radiation is much less efficient in DSB formation and produces reactive oxidative species (ROS) throughout the irradiated cell, i.e. in the nucleus, membranes, and cytoplasm. Speculating that these differences in the density of radiation and the site of energy deposition might lead to the activation of different apoptotic signaling pathways, we chose to assess cell survival and the induction of apoptosis following the decay of  $^{125}\text{I}$  specifically and selectively within the DNA of four human cell lines compared with the same endpoints following  $\gamma$ -photon irradiation.

Our studies demonstrate that the radiosensitivity of the four tumor-cell lines to DNA-incorporated  $^{125}\text{I}$  does not parallel that of  $\gamma$ -radiation. For example, whereas the RKO and LS174T cells were most radiosensitive to  $^{125}\text{I}$  (Table I), the  $D_{37}$  for LS174T cells was ~50% that of RKO cells (Table II). Although the reason(s) underlying such discord in the relative radiosensitivities of the four cell lines to these two radiation-based insults is not clear, the following differences may play a role: (i) the location and densities of the ROS produced (localized around DNA for the  $^{125}\text{I}$  decaying atoms); and (ii) dose rate effects (much higher for  $\gamma$ -irradiation).

The data also show that after  $^{125}\text{I}$ dUrd exposure, DNA laddering is induced in a dose-dependent fashion in RKO and LS174T cells (Fig. 7), indicating that apoptosis plays an important role in death in these two  $^{125}\text{I}$ -radiosensitive cell lines. On the other hand, DNA laddering is not seen in the radioresistant TE671 and MCF7 cells, suggesting that the reproductive death of these two tumor-cell lines after irradiation with  $^{125}\text{I}$ dUrd occurs almost entirely by a different mechanism (possibly necrosis). For these four tumor-cell lines, therefore, there appears to be a strong correlation between their susceptibility to apoptosis and their sensitivity to  $^{125}\text{I}$ dUrd exposure.

Consistent with the data on DNA fragmentation, after  $^{125}\text{I}$ dUrd incorporation, CASP-3 is activated rapidly and at high levels in a dose-dependent fashion in RKO and LS174T cells (Fig. 4), indicating that the pathway to apoptosis is likely signaled through the activation of CASP-3 (Table I). On the other hand, these proteases are minimally induced/activated in the TE671 rhabdomyosarcoma cells (sarcoma cell lines are not usually susceptible to apoptotic death [37]) and the *caspase-3*-gene-defective MCF7 cells [14]. Taken together with the outcome of clonogenic survival, these findings suggest that the increased  $^{125}\text{I}$ -radiosensitivity of RKO and LS174T cells may be a consequence of the activation of both cell-death pathways (apoptosis

and necrosis), whereas the lower  $^{125}\text{I}$ -radiosensitivity of TE671 and MCF7 cells may be an outcome of the activation of a post-mitotic necrotic process only. From this evidence, we conclude that the susceptibility of human tumor-cell lines to apoptosis is one of the major factors contributing to radiosensitivity following intranuclear  $^{125}\text{I}$  decay.

After  $\gamma$ -ray exposure, dose-dependent DNA laddering is observed in LS174T, RKO and MCF7 cells but not in TE671 cells (Fig. 8), and DNA fragmentation in the most  $\gamma$ -ray-radiosensitive cell line (LS174T) is more prominent than in the other cell lines. However, unlike the case with  $^{125}\text{I}$ dUrd exposure, where a clear relationship between radiosensitivity and susceptibility to apoptosis is present, such a correlation is more difficult to establish following  $\gamma$ -irradiation. While the  $D_{37}$  values in each cell type (LS174T > RKO = MCF7 > TE671) seem to be in line with the induction of DNA fragmentation (Table II), implying a good association between susceptibility to apoptosis and  $\gamma$ -radiation sensitivity, the  $D_0$  values (MCF7 > LS174T > RKO > TE671) are not. The literature is underscored by controversy on this issue. Although some reports [18,20,38] have claimed a correlation between  $\gamma$ -radiation sensitivity and the susceptibility of certain lymphoma [18], lymphoid [20,38], and fibroblast [20,38] cells to apoptosis, several studies carried out with other lymphoid cell lines [39], fibroblasts [40], and testicular germ tumor-cell lines [41] have been contradictory. These differences may be, in part, a consequence of variations in cell type, administered dose, and/or time post-irradiation (early apoptosis and delayed apoptosis), with p53-dependent pathways being thought to play an important role [13,17,42].

Within 1 h after  $\gamma$ -irradiation of cells, CASP-3 levels rise sharply (Fig. 5) in a dose-dependent fashion (Fig. 6), even though notable differences in expression between the four tumor-cell lines are observed (Table II). In agreement with accepted dogma (caspase-3 being an “executioner caspase”), it is possible to interpret these findings as indicating that apoptosis can be signaled through a CASP-3-mediated pathway in  $\gamma$ -irradiated tumor cells [43]. However, MCF7 cells have been reported by Jänicke et al. [14] to lack the expression of the *caspase-3* gene due to a 47-bp deletion within exon-3. These authors [44] also reported that  $\gamma$ -photons failed to induce apoptotic death in MCF7 cells as assessed morphologically and biochemically. In contrast, our observations demonstrate discernible and dose-dependent DNA fragmentation (i.e. apoptosis) post  $\gamma$ -irradiation of these cells (Fig. 8), possibly because of the more sensitive LM-PCR assay that we employed. Our data seem to indicate that  $\gamma$ -radiation can activate a CASP-3-independent pathway (and possibly the CASP-3-dependent pathway as well) for the induction of apoptosis in the human tumor-cell lines tested.

Our findings aid in understanding the pathways that lead to cell death following exposure to ionizing radiation. First, since the percentage of CASP-3-positive cells is always less than 50%, it is clear that postmitotic nonapoptotic mechanisms (e.g. necrosis) are predominant in cell death. Second, as neither intranuclear  $^{125}\text{I}$  decay nor  $\gamma$ -photon irradiation could activate apoptosis in one of the four human tumor-cell lines (TE671), apoptotic pathways cannot be induced in some human tumor-cell lines. Third, apoptotic cell death by DNA-incorporated Auger electron emitters seems to be selectively induced through a CASP-3-mediated pathway and correlates with cellular radiosensitivity. The induction of apoptosis by  $\gamma$ -radiation, on the other hand, can be initiated through either CASP-3-independent or CASP-3-mediated pathways. We postulate that these differences between  $^{125}\text{I}$ dUrd and  $\gamma$ -radiation are a consequence of (i) the genetic make up of the tumor cells, (ii) the location within the cell from which the signal originates, (iii) the nature of the radiation insult, and (iv) the radiosensitivity of the tumor cells. Further studies will continue to clarify these important factors.

## Conclusions

- Radiosensitivities of four tumor cell lines to  $\gamma$ -irradiation do not necessarily parallel those to  $^{125}\text{I}$  decay.
- Apoptotic cell death after  $\gamma$ -irradiation is probably initiated via CASP-3-independent and/or CASP-3-mediated pathways and does not seem to correlate with cell radiosensitivity.
- Apoptotic cell death initiated by DNA-incorporated  $^{125}\text{I}$  is dose-dependent, correlates with radiation sensitivity, and seems to occur only through the CASP-3-mediated pathway.
- DNA fragmentation is not detected when less than 10% of cells are positive for CASP-3.
- Differences in the nature of the radiation emitted and in the sites of energy deposition appear to activate distinct pathways that lead to the induction of apoptosis.
- After exposure to ionizing radiation, postmitotic nonapoptotic mechanisms (e.g. necrosis) are predominant in clonogenic cell death.
- Apoptosis cannot be induced in all tumor cell lines.

## Acknowledgements

This work was supported by NIH Grant 5 R01 CA15523 (to A. I. K.).

## References

1. Kerr JFR, Wyllie AH, Currie AR. Apoptosis: a basic biological phenomenon with wide-ranging implications in tissue kinetics. *Br J Cancer* 1972;26:239–57. [PubMed: 4561027]
2. Dewey WC, Ling CC, Meyn RE. Radiation-induced apoptosis: relevance to radiotherapy. *Int J Radiat Oncol Biol Phys* 1995;33:781–96. [PubMed: 7591884]
3. Alnemri ES, Livingston DJ, Nicholson DW, et al. Human ICE/CED-3 protease nomenclature. *Cell* 1996;87:171. [PubMed: 8861900]
4. Thornberry NA, Rano TA, Peterson EP, et al. A combinatorial approach defines specificities of members of the caspase family and granzyme B: functional relationships established for key mediators of apoptosis. *J Biol Chem* 1997;272:17907–11. [PubMed: 9218414]
5. Thornberry NA, Lazebnik Y. Caspases: enemies within. *Science* 1998;281:1312–6. [PubMed: 9721091]
6. Lazebnik YA, Kaufmann SH, Desnoyers S, Poirier GG, Earnshaw WC. Cleavage of poly(ADP-ribose) polymerase by a proteinase with properties like ICE. *Nature* 1994;371:346–7. [PubMed: 8090205]
7. Casciola-Rosen LA, Anhalt GJ, Rosen A. DNA-dependent protein kinase is one of a subset of autoantigens specifically cleaved early during apoptosis. *J Exp Med* 1995;182:1625–34. [PubMed: 7500007]
8. Nicholson DW, Ali A, Thornberry NA, et al. Identification and inhibition of the ICE/CED-3 protease necessary for mammalian apoptosis. *Nature* 1995;376:37–43. [PubMed: 7596430]
9. Song Q, Lees-Miller SP, Kumar S, et al. DNA-dependent protein kinase catalytic subunit: a target for an ICE-like protease in apoptosis. *EMBO J* 1996;15:3238–46. [PubMed: 8670824]
10. Liu X, Zou H, Slaughter C, Wang X. DFF, a heterodimeric protein that functions downstream of caspase-3 to trigger DNA fragmentation during apoptosis. *Cell* 1997;89:175–84. [PubMed: 9108473]
11. Jänicke RU, Ng P, Sprengart ML, Porter AG. Caspase-3 is required for  $\alpha$ -fodrin cleavage but dispensable for cleavage of other death substrates in apoptosis. *J Biol Chem* 1998;273:15540–5. [PubMed: 9624143]
12. Datta R, Kojima H, Banach D, et al. Activation of a CrmA-insensitive, p35-sensitive pathway in ionizing radiation-induced apoptosis. *J Biol Chem* 1997;272:1965–9. [PubMed: 8999887]

13. Yu Y, Little JB. p53 is involved in but not required for ionizing radiation-induced caspase-3 activation and apoptosis in human lymphoblast cell lines. *Cancer Res* 1998;58:4277–81. [PubMed: 9766652]
14. Jänicke RU, Sprengart ML, Wati MR, Porter AG. Caspase-3 is required for DNA fragmentation and morphological changes associated with apoptosis. *J Biol Chem* 1998;273:9357–60. [PubMed: 9545256]
15. Yamada T, Ohyama H. Radiation-induced interphase death of rat thymocytes is internally programmed (apoptosis). *Int J Radiat Biol* 1988;53:65–75.
16. Palayoor ST, Humm JL, Atcher RW, Hines JJ, Macklis RM. G2M arrest and apoptosis in murine T lymphoma cells following exposure to <sup>212</sup>Bi alpha particle irradiation. *Nucl Med Biol* 1993;20:795–805. [PubMed: 8401380]
17. Radford IR, Murphy TK, Radley JM, Ellis SL. Radiation response of mouse lymphoid and myeloid cell lines. Part II. Apoptotic death is shown by all lines examined. *Int J Radiat Biol* 1994;65:217–27. [PubMed: 7907119]
18. Story MD, Voehringer DW, Malone CG, Hobbs ML, Meyn RE. Radiation-induced apoptosis in sensitive and resistant cells isolated from a mouse lymphoma. *Int J Radiat Biol* 1994;66:659–68. [PubMed: 7814966]
19. Meijer AE, Kronqvist U-SE, Lewensohn R, Harms-Ringdahl M. RBE for the induction of apoptosis in human peripheral lymphocytes exposed *in vitro* to high-LET radiation generated by accelerated nitrogen ions. *Int J Radiat Biol* 1998;73:169–77. [PubMed: 9489564]
20. Radford IR, Aldridge DR. Importance of DNA damage in the induction of apoptosis by ionizing radiation: effect of the *scid* mutation and DNA ploidy on the radiosensitivity of murine lymphoid cell lines. *Int J Radiat Biol* 1999;75:143–53. [PubMed: 10072175]
21. Meijer AE, Ekedahl J, Joseph B, et al. High-LET radiation induces apoptosis in lymphoblastoid cell lines derived from ataxia-telangiectasia patients. *Int J Radiat Biol* 2001;77:309–17. [PubMed: 11258845]
22. Charlton DE, Booz J. A Monte Carlo treatment of the decay of <sup>125</sup>I. *Radiat Res* 1981;87:10–23. [PubMed: 7255664]
23. Sastry, KSR.; Rao, DV. Dosimetry of low energy electrons. In: Rao, DV.; Chandra, R.; Graham, MC., editors. *Physics of nuclear medicine: recent advances*. Woodbury, NY: American Institute of Physics; 1984. p. 169-208.
24. Kassis AI, Sastry KSR, Adelstein SJ. Kinetics of uptake, retention, and radiotoxicity of <sup>125</sup>IuDR in mammalian cells: implications of localized energy deposition by Auger processes. *Radiat Res* 1987;109:78–89. [PubMed: 3809393]
25. Kassis AI, Fayad F, Kinsey BM, Sastry KSR, Taube RA, Adelstein SJ. Radiotoxicity of <sup>125</sup>I in mammalian cells. *Radiat Res* 1987;111:305–18. [PubMed: 3628718]
26. Kassis AI. The amazing world of Auger electrons. *Int J Radiat Biol* 2004;80:789–803. [PubMed: 15764386]
27. Keough G, Hofer KG. Molecular consequences of the Auger effect: the fate of iododeoxyuridine following iodine-125 decay. *Radiat Res* 1976;67:224–34. [PubMed: 948550]
28. Deutzmann R, Stöcklin G. Chemical effects of iodine-125 decay in aqueous solution of 5-iodouracil. Ring fragmentation as a consequence of the Auger effect. *Radiat Res* 1981;87:24–36. [PubMed: 6789368]
29. Martin RF, Haseltine WA. Range of radiochemical damage to DNA with decay of iodine-125. *Science* 1981;213:896–8. [PubMed: 7256283]
30. Kassis AI, Harapanhalli RS, Adelstein SJ. Comparison of strand breaks in plasmid DNA after positional changes of Auger electron-emitting iodine-125. *Radiat Res* 1999;151:167–76. [PubMed: 9952301]
31. Hofer KG, Hughes WL. Radiotoxicity of intranuclear tritium, <sup>125</sup>iodine and <sup>131</sup>iodine. *Radiat Res* 1971;47:94–109. [PubMed: 5559387]
32. Chan PC, Lisco E, Lisco H, Adelstein SJ. The radiotoxicity of iodine-125 in mammalian cells. II. A comparative study on cell survival and cytogenetic responses to <sup>125</sup>IuDR, <sup>131</sup>IuDR, and <sup>3</sup>H. *Radiat Res* 1976;67:332–43.



33. Walicka MA, Adelstein SJ, Kassis AI. Indirect mechanisms contribute to biological effects produced by decay of DNA-incorporated iodine-125 in mammalian cells *in vitro*: double-strand breaks. *Radiat Res* 1998;149:134–41. [PubMed: 9457892]
34. Kassis AI, Walicka MA, Adelstein SJ. Double-strand break yield following  $^{125}\text{I}$  decay: *effects of DNA conformation*. *Acta Oncol* 2000;39:721–6. [PubMed: 11130010]
35. Hofer KG, Harris CR, Smith JM. Radiotoxicity of intracellular  $^{67}\text{Ga}$ ,  $^{125}\text{I}$  and  $^3\text{H}$ : nuclear versus cytoplasmic radiation effects in murine L1210 leukaemia. *Int J Radiat Biol* 1975;28:225–41.
36. Warters RL, Hofer KG, Harris CR, Smith JM. Radionuclide toxicity in cultured mammalian cells: elucidation of the primary site of radiation damage. *Curr Top Radiat Res Q* 1977;12:389–407. [PubMed: 565271]
37. Hall, EJ. *Radiobiology for the radiologist*. fourth ed. Philadelphia: JB Lippincott Company; 1994.
38. Rupnow BA, Murtha AD, Alarcon RM, Giaccia AJ, Knox SJ. Direct evidence that apoptosis enhances tumor responses to fractionated radiotherapy. *Cancer Res* 1998;58:1779–84. [PubMed: 9581811]
39. Jaworska A, Szumiel I, De Angelis P, Olsen G, Reitan J. Evaluation of ionizing radiation sensitivity markers in a panel of lymphoid cell lines. *Int J Radiat Biol* 2001;77:269–80. [PubMed: 11258841]
40. Aldridge DR, Arends MJ, Radford IR. Increasing the susceptibility of the rat 208F fibroblast cell line to radiation-induced apoptosis does not alter its clonogenic survival dose – response. *Br J Cancer* 1995;71:571–7. [PubMed: 7880740]
41. Burger H, Nooter K, Boersma AWM, Kortland CJ, van den Berg AP, Stoter G. Expression of p53, p21/WAF/CIP, Bcl-2, Bax, Bcl-x, and Bak in radiation-induced apoptosis in testicular germ cell tumor lines. *Int J Radiat Oncol Biol Phys* 1998;41:415–24. [PubMed: 9607360]
42. Clarke AR, Purdie CA, Harrison DJ, et al. Thymocyte apoptosis induced by p53-dependent and independent pathways. *Nature* 1993;362:849–52. [PubMed: 8479523]
43. Urashima T, Wang K, Adelstein SJ, Kassis AI. Activation of diverse pathways to apoptosis by  $^{125}\text{I}$ Urd and  $\gamma$ -photon exposure. *Int J Radiat Biol* 2004;80:867–74. [PubMed: 15764395]
44. Jänicke RU, Engels IH, Dunkern T, Kaina B, Schulze-Osthoff K, Porter AG. Ionizing radiation but not anticancer drugs causes cell cycle arrest and failure to activate the mitochondrial death pathway in MCF-7 breast carcinoma cells. *Oncogene* 2001;20:5043–53. [PubMed: 11526489]

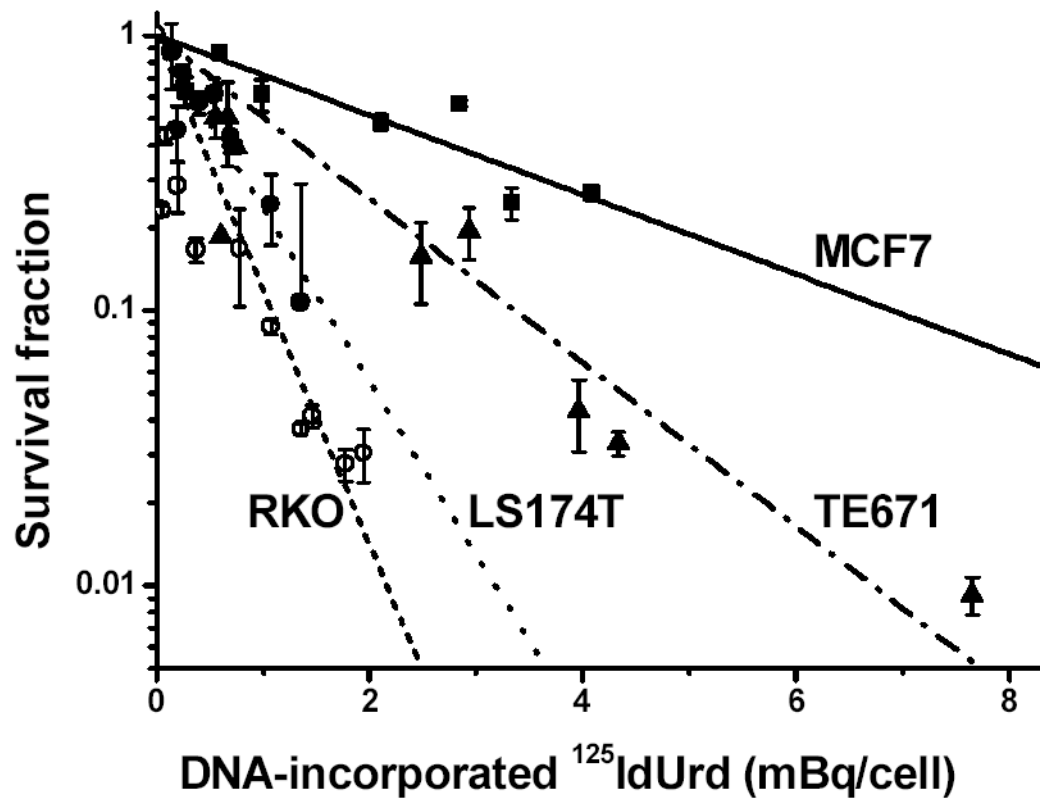


**Figure 1.** Clonogenic survival of tumor cells exposed to various radioactive concentrations of  $^{125}\text{I}$ IdUrd for 48 h at  $37^\circ\text{C}$ . Survival fraction is plotted as a function of DNA-incorporated  $^{125}\text{I}$  activity (mBq/cell). Linear regressions of data points  $\pm$  SD were generated using Origin 7.0 (OriginLab, Northampton, MA).

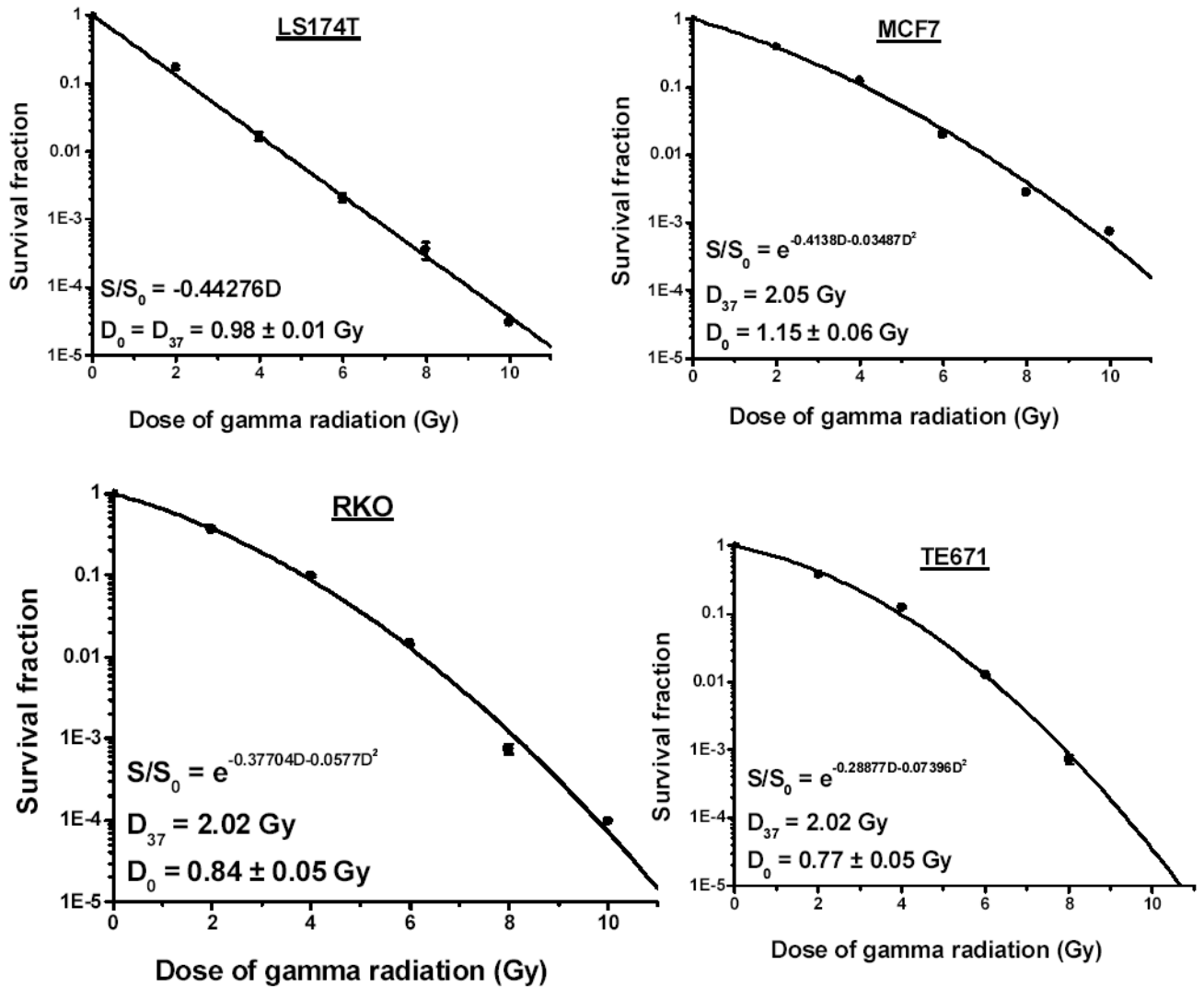


**Figure 2.** Clonogenic survival of tumor cells exposed to various doses of  $\gamma$ -ray radiation. Survival fraction is plotted as function of dose (Gy). Data points  $\pm$  SD were fitted (second order polynomial) using Origin 7.0 (OriginLab, Northampton, MA).

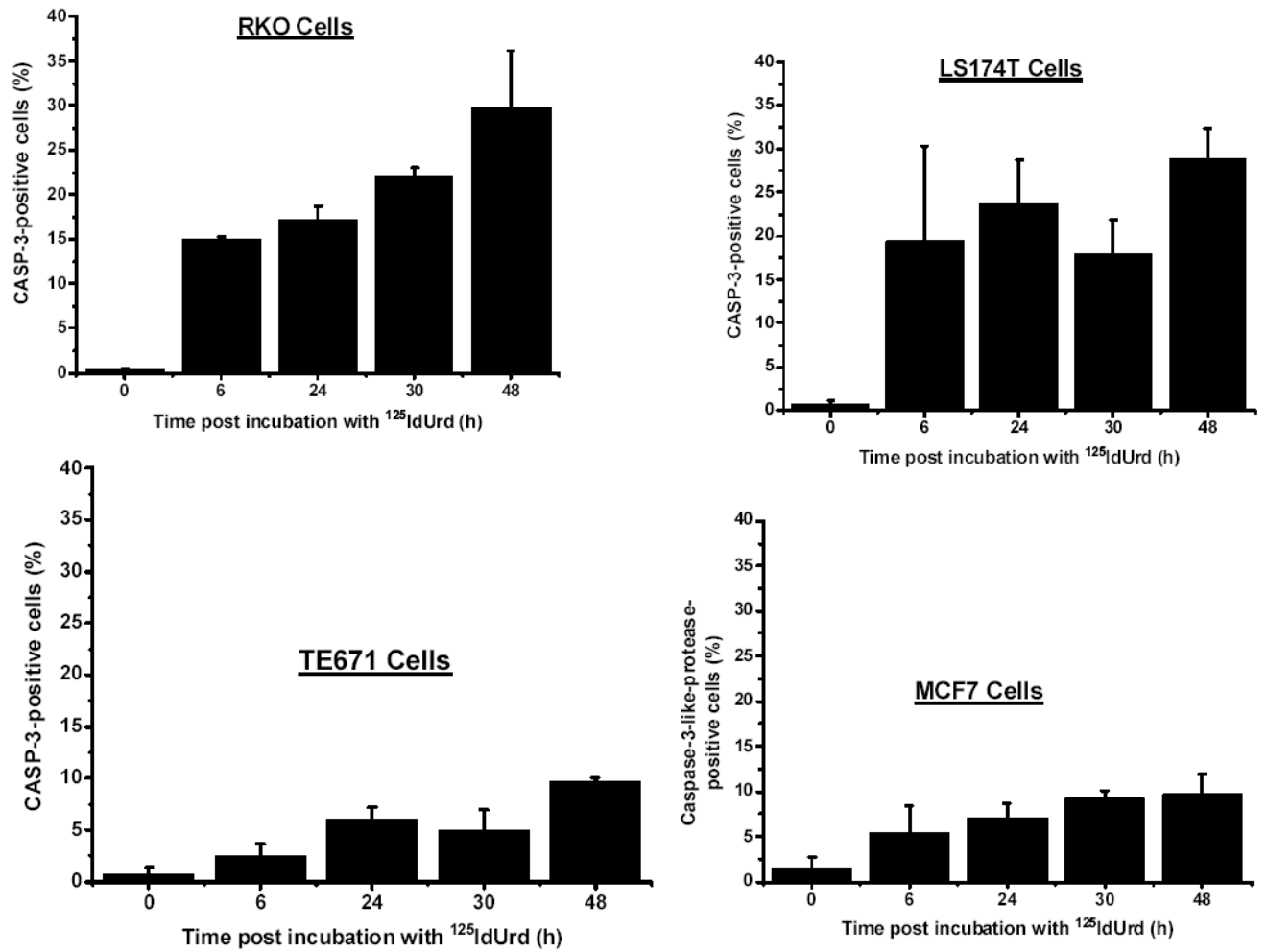


**Figure 3.** Caspase-3 expression in tumor cells at various times after 48-h incubation with  $^{125}\text{IIdUrd}$  (37 kBq/ml). Cells were incubated with fluorogenic substrate and percentage of cells positive for caspase-3 was determined under fluorescence microscope.

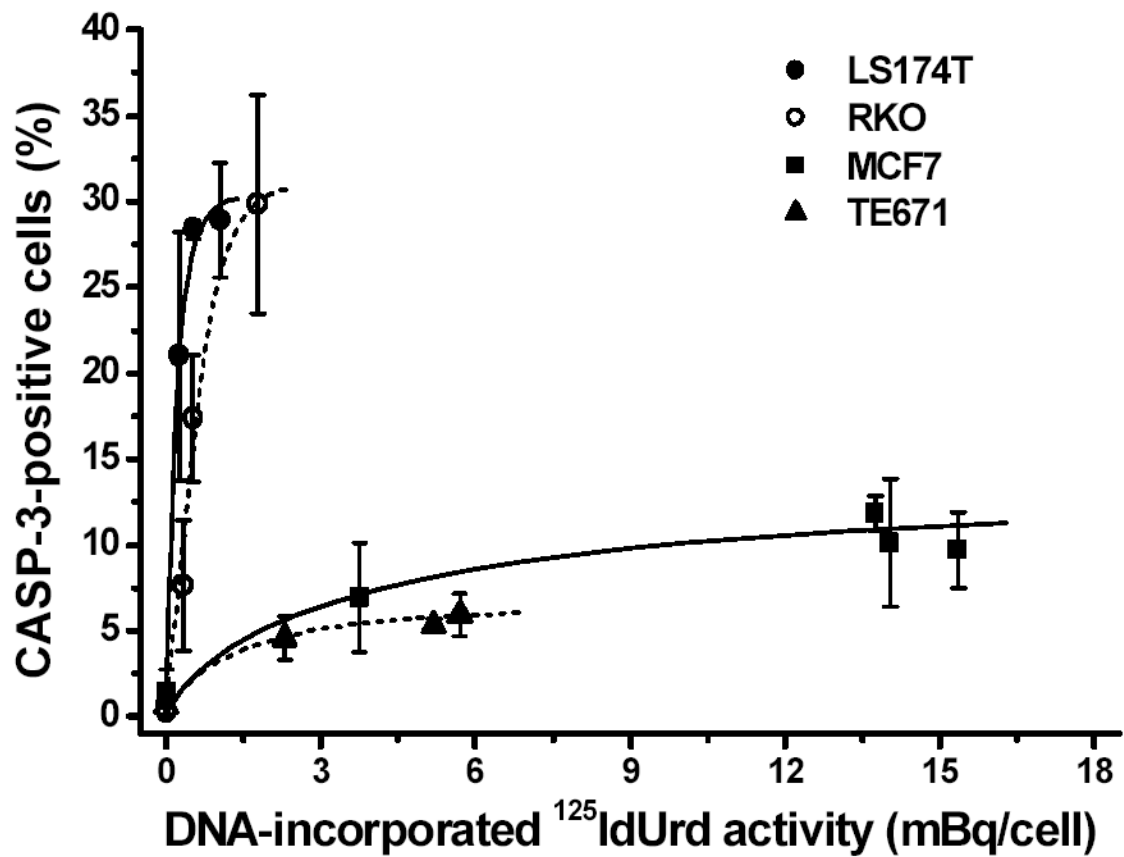


**Figure 4.** Caspase-3 expression in tumor cells exposed to various radioactive concentrations of  $^{125}\text{I}$ IdUrd for 48 h at 37°C. Cells were incubated with fluorogenic substrate and percentage of cells positive for caspase-3 was determined under fluorescence microscope and plotted as function of DNA-incorporated  $^{125}\text{I}$  activity (mBq/cell). Data points  $\pm$  SD were fitted by hand.

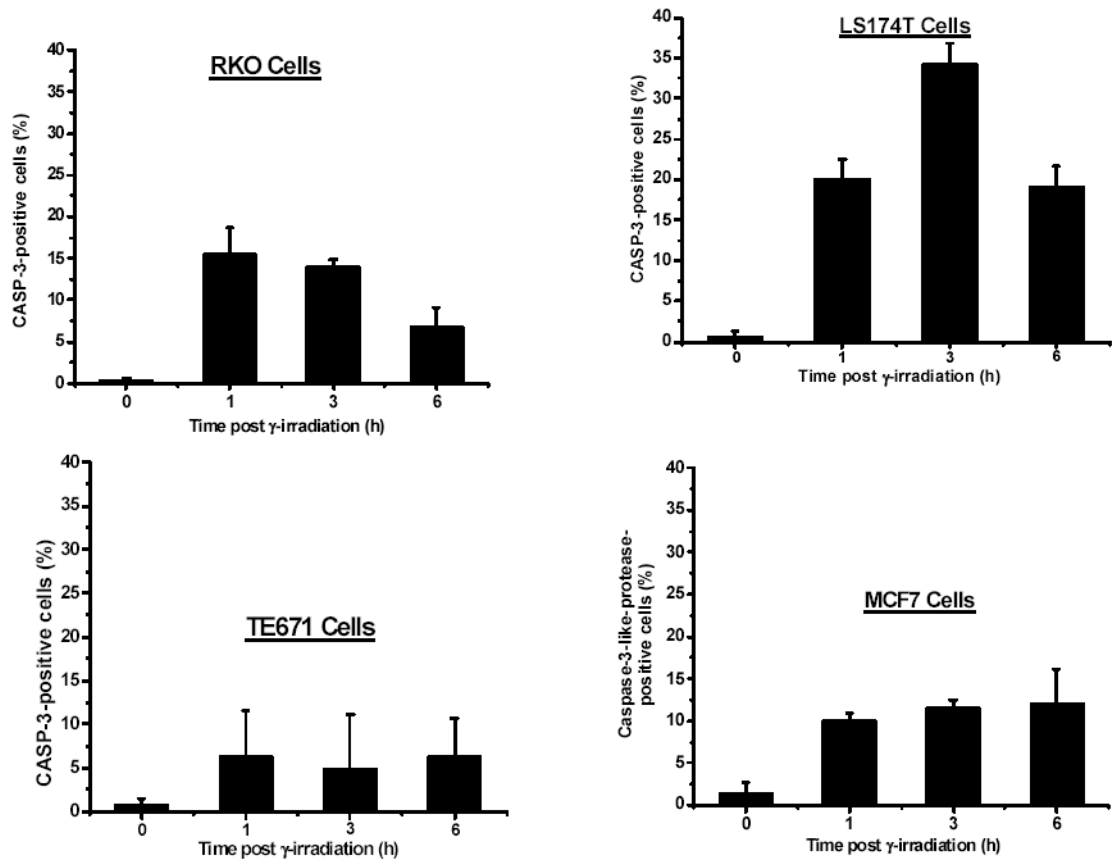


**Figure 5.** Caspase-3 expression in tumor cells at various times after exposure to  $\gamma$ -radiation (5 Gy). Cells were incubated with fluorogenic substrate and percentage of cells positive for caspase-3 was determined under fluorescence microscope.

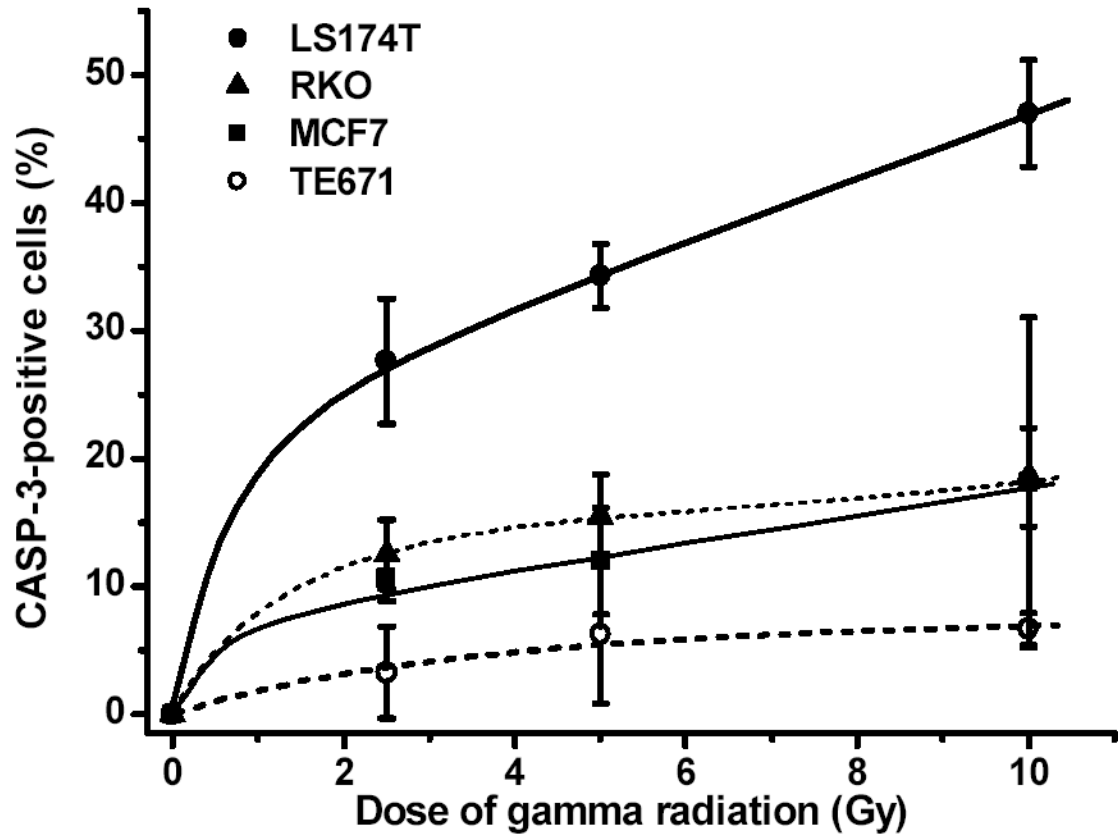


**Figure 6.**

Caspase-3 expression in tumor cells exposed to various doses of  $\gamma$ -radiation. Percentage of cells positive for caspase-3 was determined at time points when endonuclease levels were highest (RKO cells, 1 h; LS174T cells, 3 h; TE671 and MCF7 cells, 6 h).

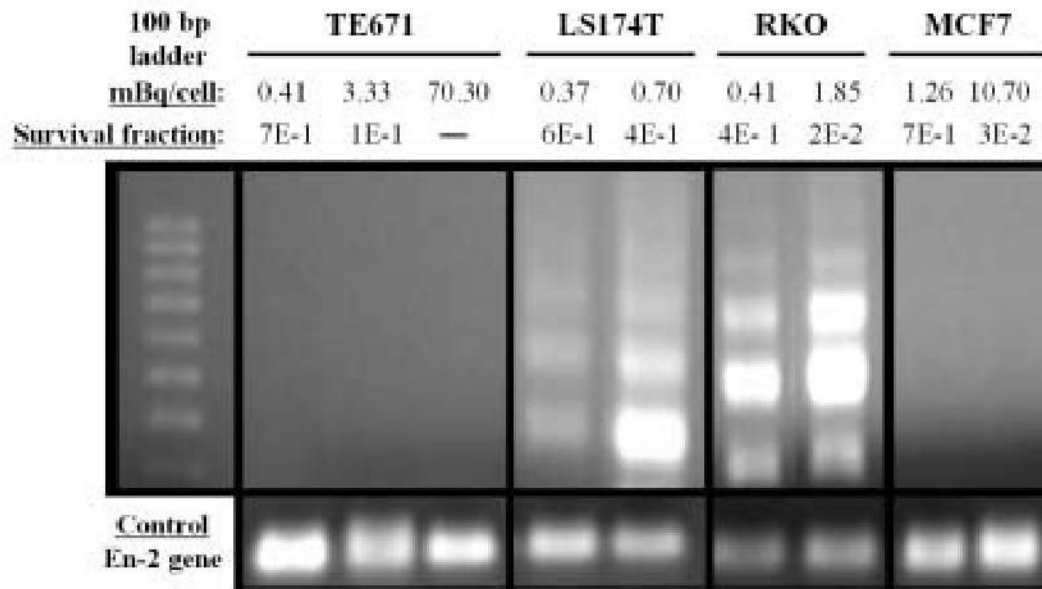


**Figure 7.** Detection of DNA fragmentation by LM-PCR in TE671, LS174T, RKO, and MCF7 cells incubated for 48 h with various concentrations of <sup>125</sup>I dUrd. Upper panel: Left lane contains molecular weight markers. DNA-incorporated <sup>125</sup>I activity (mBq/cell) and survival fractions are shown. Lower panel: *En-2*, a single-copy gene that is conserved in most species, has been run as control (same amount of DNA used).



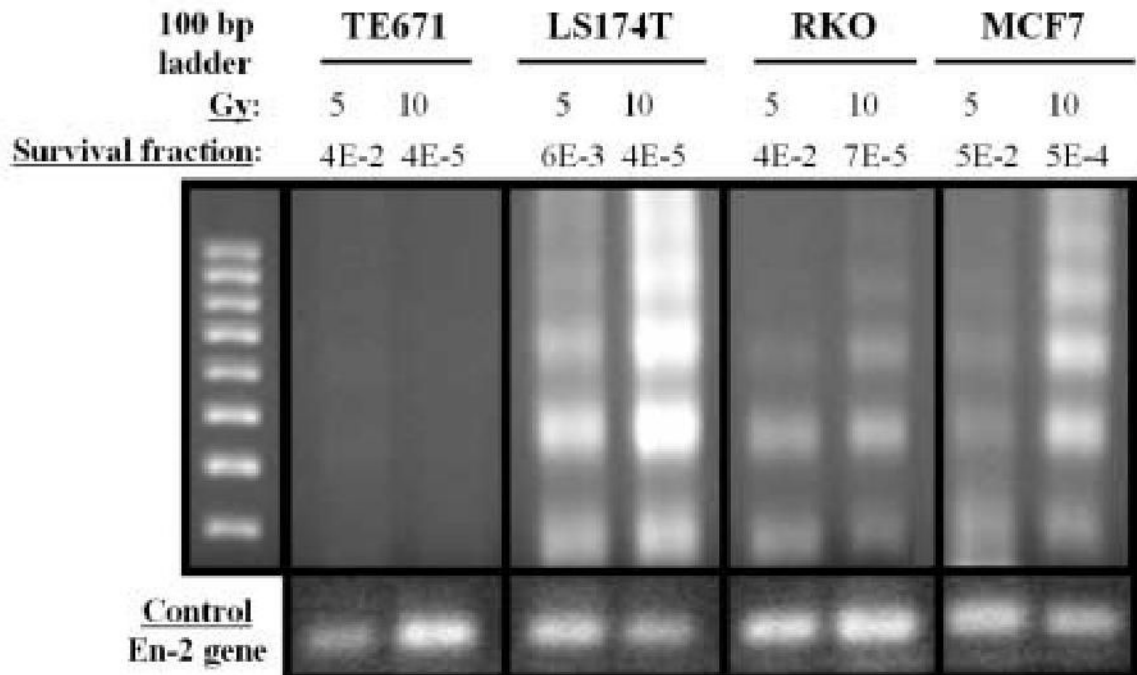


**Figure 8.** Detection of DNA fragmentation by LM-PCR in TE671, LS174T, RKO, and MCF7 cells 6 h after  $\gamma$ -ray irradiation. Upper panel: Left lane contains molecular weight markers. Dose of  $\gamma$ -radiation (Gy) and survival fractions are shown. Lower panel: *En-2*, a single-copy gene that is conserved in most species, has been run as control (same amount of DNA used).